Ecological Indicators 96 (2019) 448–457

Contents lists available at ScienceDirect

Ecological Indicators

journal homepage: www.elsevier.com/locate/ecolind

Original Articles

sc_PDSI is more sensitive to precipitation than to reference evapotranspiration in China during the time period 1951–2015

Yajie Zhang[a], Gaopeng Li[b], Jing Ge[b], Yao Li[a], Zhisheng Yu[a], Haishan Niu[a,*]

[a] College of Resources and Environment, University of Chinese Academy of Sciences, No. 19A Yuquan Road, Beijing, China
[b] Shanghai Institutes for Biological Sciences, Chinese Academy of Sciences, No. 320 Yueyang Road, Shanghai, China

ARTICLE INFO

Keywords:
sc_PDSI
Precipitation
Reference evapotranspiration
Detrending
China

ABSTRACT

The self-calibrating Palmer Drought Severity Index (sc_PDSI) is developed within the frame of the PDSI model, but is considered to be more appropriate for global drought monitoring. The sc_PDSI can automatically calibrate itself at any location using dynamically computed values and can calculate evapotranspiration using the FAO-56 Penman–Monteith (P–M) equation. However, the correlation of the sc_PDSI(P–M) with some factors that drive drought, such as precipitation (P) and the reference evapotranspiration (ET_0), is still unclear in China. With the aim of solving this issue, we analyzed the correlation of the detrended sc_PDSI(P–M) with the detrended P and ET_0 on different timescales (one, three, six and 12 months) in China for the period 1951–2015. The results show that both the P and ET_0 are highly correlated with the sc_PDSI(P–M) on a 12-month timescale. On this timescale, the sc_PDSI(P–M) is more sensitive to P than to ET_0 on the national scale, except for northeastern China. Thus the sc_PDSI(P–M) may effectively fit the long-term variations in these drivers of drought, especially P. These results provide guidance on the use of the sc_PDSI(P–M) to detect the impacts of climate change on drought severity under the climatic conditions found in China.

1. Introduction

Extreme climate and weather events cause significant disruption to human societies and anthropogenic climate change is expected to increase the occurrence, magnitude and/or impact of these events in the future (Coumou and Rahmstorf, 2012). Drought is an extreme phenomenon caused by low and irregular precipitation and high rates of evapotranspiration over an extended period of time. Droughts have long-term impacts on crucial water resources, agricultural production and socioeconomic activities (Hanson, 1991; Ding et al, 2011). China is affected by frequent and severe droughts and historical records show that large-scale droughts have occurred many times, although the situation has deteriorated since the 1990s (Zou et al., 2005; Shen et al., 2007; Dai, 2011a,b; Miyan, 2015). Nationwide droughts now occur almost every year and cause severe famine, water shortages, desertification and dust storms in many areas (Zhang, 2003; Dai et al., 2004; Zou et al., 2005; Zhai et al., 2010). Monitoring the variations and trends in droughts could provide important information for use as a reference in improving the management of agricultural production, water resources and in the prediction of disasters (Zhao et al., 2015; Zhang et al., 2017).

Droughts are a result of the integrated effects of multiple factors, such as precipitation, evapotranspiration and total water storage (Yu and Gao, 1991). In meteorology, precipitation (P) is defined as any product of the condensation of atmospheric water vapor that falls under gravity, whereas evapotranspiration is the sum of evaporation and plant transpiration from the Earth's land and ocean surfaces to the atmosphere. In agricultural applications, the actual evapotranspiration of crops can be derived from the reference evapotranspiration (ET_0), which indicates the environmental demand for evapotranspiration and represents the evapotranspiration rate of a short green crop (grass) that completely shades the ground, is of uniform height and has an adequate water status in the soil profile using the correct crop and water stress coefficients (Kite and Droogers, 2000; Rana and Katerji, 2000). Several equations are available for estimating ET_0 (e.g., Penman, 1948; Blaney and Criddle, 1950; Hargreaves and Samani, 1985). Among these, the FAO-56 Penman–Monteith (P–M) equation, which incorporates both energy balance and aerodynamic theory, is considered to be the most appropriate model to predict ET_0 and is recommended by the Food and Agriculture Organization of the United Nations as the standard for computing ET_0 from full climate records (Allen et al., 1998). As major components of the water cycle, P and ET_0 are always considered as factors that indicate the degree and determine the duration of drought (Heim, 2002).

* Corresponding author.
E-mail address: niuhs@ucas.ac.cn (H. Niu).

https://doi.org/10.1016/j.ecolind.2018.09.033
Received 7 January 2017; Received in revised form 7 September 2018; Accepted 14 September 2018
Available online 20 September 2018

Fig. 1. Topographic and geographical zones of China (modified from Zhang et al. (2018)).

Numerous drought indices have been developed to quantify complicated drought processes and to manifest the actual hydrological conditions in a single number (Wilhite and Glantz, 1985; Heim, 2002). Drought indices can be classified as precipitation indices, water budget indices, soil moisture indices, hydrological indices and aridity indices, all of which indicate the moisture conditions and the deficiency or surplus of water for a given area from different points of view (Szép et al., 2005). One of the most commonly used indices is the Palmer Drought Severity Index (PDSI), which uses precipitation, temperature and the local available water content to assess the precipitation deficit/surplus with respect to a value that is climatologically appropriate for the existing conditions in a given region (Palmer, 1965). In the PDSI, the water balance is calculated using a two-layer bucket-type model in which the soil fills with precipitation and empties through actual evapotranspiration and runoff on a monthly timescale (Hobbins et al., 2008). The range of values of the PDSI is between −4 and +4. Negative (positive) PDSI values indicate dry (wet) periods, whereas those near zero presume a near-average state (Palmer, 1965). The PDSI provides a comprehensive method with which to assess the impact of climate change on drought on a monthly basis because it requires specific climate variables as inputs and is intended to be of reasonably comparable local significance in both space and time (Heim, 2002; Dai et al., 2004; Sheffield et al., 2012; Vicente-Serrano et al., 2012; van der Schrier et al., 2013; Zoljoodi and Didevarasl, 2013). However, as a result of the application of weighting and duration factors derived from empirical calibrations against a limited amount of data observed over the US Great Plains, the PDSI has proved to be unsuitable for applications in different climatological regions (Palmer, 1965; Liu et al, 2004). To solve this drawback, the self-calibrating PDSI (sc_PDSI) model, which automatically calibrates itself at any location using dynamically computed values, was developed within the frame of the PDSI model and is considered to be more appropriate for global drought monitoring (Wells et al., 2004; Dai, 2011a,b; van der Schrier et al., 2011, 2013). In the traditional formulation of the PDSI, evaporative demand is derived from an approach that can be traced back to Thornthwaite (1948) and is solely a function of air temperature. However, the evapotranspiration calculated using the FAO-56 Penman–Monteith equation, which incorporates both the energy balance and aerodynamic theory, is now considered to be more appropriate (Penman, 1948; Allen et al., 1998; van der Schrier et al., 2011; Sheffield et al., 2012; Trenberth et al., 2014). Many studies have been conducted in China to evaluate and apply different drought indices and the PDSI (P–M) and sc_PDSI(P–M) are considered to be the best indices of drought (Wei and Ma, 2003; Lu et al., 2015).

The standardized precipitation index and standardized precipitation evapotranspiration index are both sensitive to the factors driving drought (e.g., the standardized precipitation evapotranspiration index shows equal sensitivity to P and ET_0) (Guttman, 1998; Hayes et al., 1999, 2000; Vicente-Serrano et al., 2012, 2015). However, there have been insufficient studies focused on the correlation of the sc_PDSI(P–M) with variations in P and ET_0. Hu and Willson (2000) showed that the PDSI is equally affected by temperature and precipitation when both have similar magnitudes of anomalies. Vicente-Serrano et al. (2015) showed that the PDSI was not equally sensitive to P and ET_0 and the

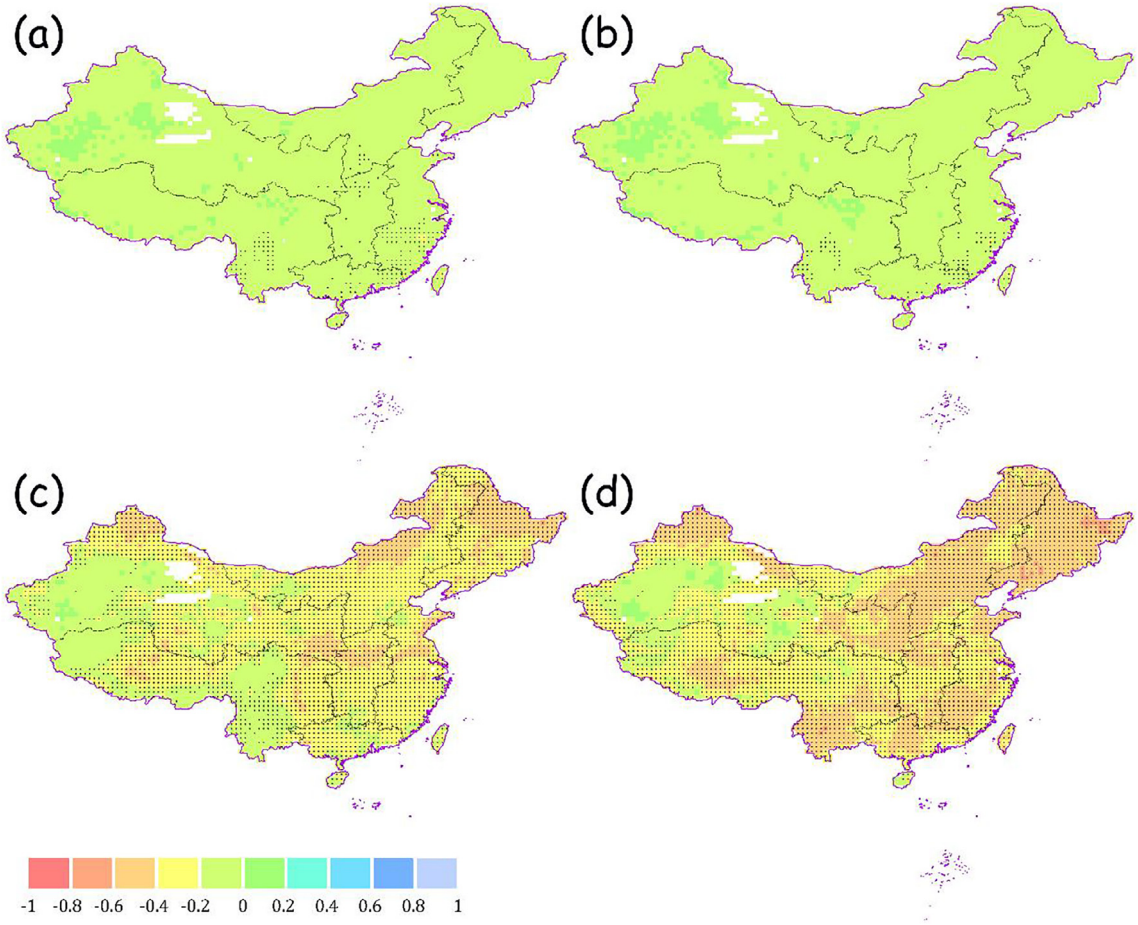

Fig. 2. Pearson's correlation coefficient between the self-calibrating Palmer Drought Severity Index using the FAO-56 Penman–Monteith equation (sc_PDSI(P–M)) and reference evapotranspiration (ET_0) on different timescales at the grid cell level in China during 1951–2015. The dotted areas are statistically significant at the 5% level. (a) One-month, (b) three-month, (c) six-month and (d) 12-month timescales.

differences in the means and standard deviations of P and ET_0 determined the sensitivity of the PDSI. The sc_PDSI does not relate to a specific timescale and can be qualified as a medium to long timescale drought monitoring index and therefore the correlation of the sc_PDSI (P–M) with P and ET_0 needs to be evaluated on different timescales. Few studies have been carried out in China, which may affect the application of the PDSI and sc_PDSI in this region. We therefore analyzed the relative contribution of variations in P and ET_0 to the spatial and temporal variability of sc_PDSI(P–M). We aimed to: (1) conduct a simple analysis of the correlation of the sc_PDSI(P–M) with variations in P and ET_0 at the grid cell level; (2) evaluate the different timescales of P and ET_0 that are highly correlated with the sc_PDSI(P–M); (3) determine the influence of P and ET_0 on the sc_PDSI(P–M); and (4) provide advice on the use of the sc_PDSI(P–M) to detect droughts and plan the utilization of water resources in China and other countries or regions with similar climatic and geographical conditions. This research may also provide a theoretical basis for the application of the sc_PDSI (P–M) to detect the impact of climate change on the severity of drought in China.

2. Data and methods

2.1. Data sources and processing

Global monthly P, ET_0 and sc_PDSI data were used to analyze the correlation between the sc_PDSI(P–M) and P and ET_0 (P–M). These data are published by the Climatic Research Unit, University of East Anglia as the TS3.24 dataset (Harris et al., 2014; www.cru.uea.ac.uk/data/; last accessed 2016) with a spatial resolution of 0.5° × 0.5°. The dataset covers the period from January 1951 to December 2015. ET_0 in the TS3.24 dataset is obtained using the FAO-56 Penman–Monteith equation. The sc_PDSI in the TS3.24 dataset is calculated from time series of precipitation and temperature and fixed parameters related to the soil/surface characteristics at each location (van der Schrier et al., 2013).

Version 3.3.1 of R software (Statistics Department of the University of Auckland; www.r-project.org/) was used to resample and clip the sc_PDSI(P–M), P and ET_0 data to the same spatial resolution of 0.5° × 0.5° and the same spatial extent in the time range January 1951 to December 2015. The monthly P and ET_0 datasets were aggregated and processed to different timescales (three, six and 12 months) using an accumulating method. R was then applied to conduct Pearson's correlation analysis and standardized regression analysis for these three factors (and the detrended factors) to obtain the correlation coefficients, regression coefficients and their corresponding p values at the 95% confidence level. The R packages used in these calculation procedures mainly contain "raster", "ncdf4", "lattice", "lm.beta" and "car". The differences between the means of the Pearson's correlation coefficients of the sc_PDSI(P–M) and those of P and ET_0 (and of the detrended sc_PDSI(P–M) with the detrended P and ET_0) data on different timescales were analyzed using one-way ANOVA in IBM SPSS Statistics 20. Normality was tested using the Shapiro–Wilk method and the homogeneity of variance was tested during the one-way ANOVA. Data transformations were not required. Significance was accepted when H_0 was rejected at a probability of $p \leq 0.05$. Microsoft Excel 2013 was also used for data manipulation. After the results had been derived, ArcGIS (version 10.1) was used for data visualization. The significance levels

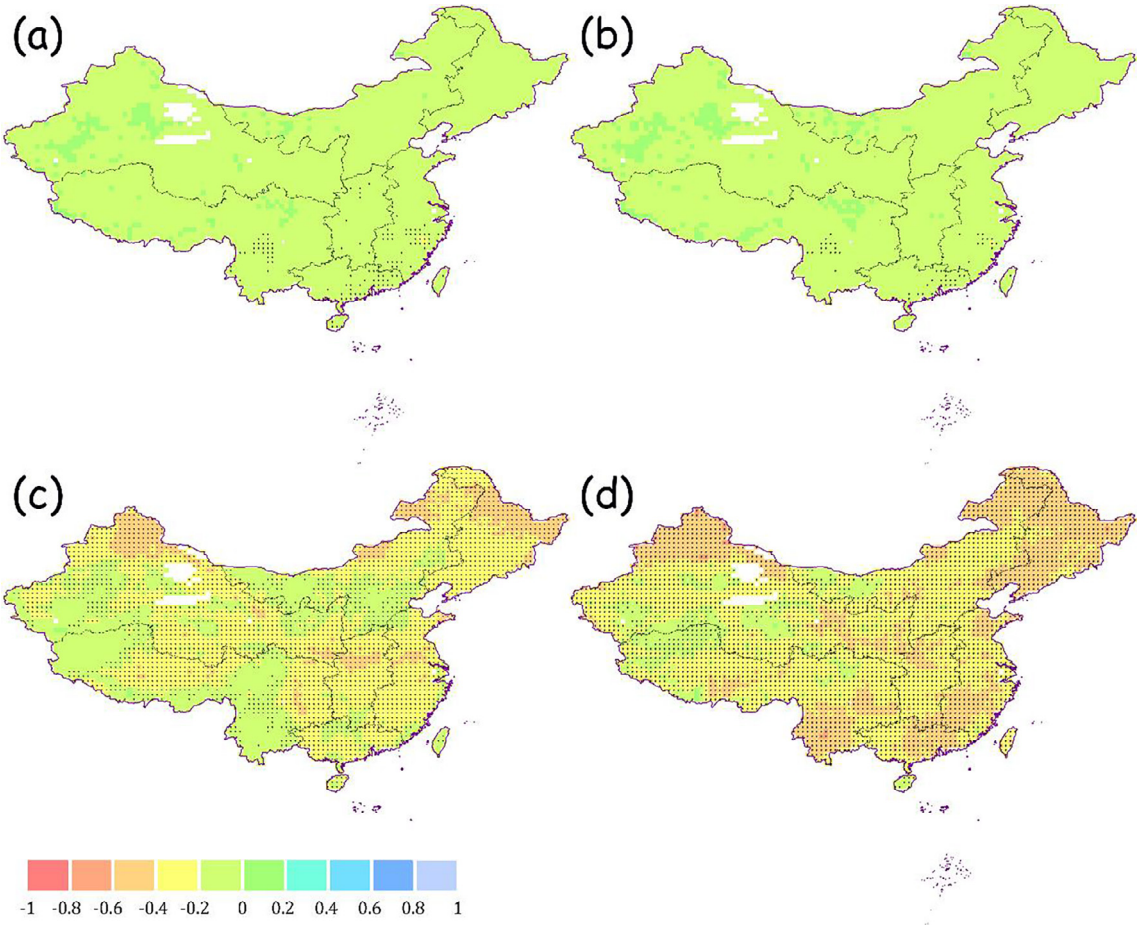

Fig. 3. Pearson's correlation coefficient between the detrended self-calibrating Palmer Drought Severity Index using the FAO-56 Penman–Monteith equation (sc_PDSI (P–M)) and detrended reference evapotranspiration (ET_0) on different timescales at the grid cell level in China during 1951–2015. The dotted areas are statistically significant at the 5% level. (a) One-month, (b) three-month, (c) six-month and (d) 12-month timescales.

were $p \leq 0.05$.

The natural geographical division method was used to divide China into seven regions: northeast, north, east, central, south, northwest and southwest (Fig. 1).

2.2. Methodology

2.2.1. Pearson's correlation analysis and standardized multiple regression analysis

Different attribution analysis methods have been used to evaluate the contributions of climate factors to variations in drought indices. The most commonly used methods are correlation analysis and multiple regression analysis (Vicente-Serrano et al., 2015). The spatial correlation between the sc_PDSI(P–M) and the factors driving drought (and between the detrended sc_PDSI(P–M) and factors driving drought) was examined by calculating Pearson's correlation coefficient and the standardized multiple regression coefficient using all land grid cells (Xu et al., 2006; Nouri et al., 2017).

2.2.2. MK trend test

The MK trend test has been widely used for trend detection in hydrology and climatology time series as a result of its rank-based procedure with resistance to the influence of the extreme values that facilitate skewness variables (Bihrat and Bayazit, 2003). The presence of a statistically significant trend is evaluated using the MK test statistic Z value. If $Z > 0$, the time series has an upward trend and if $Z < 0$ it has a downward trend. The critical value of Z at the $\alpha = 5\%$ significance level of the trend test is equal to 1.96. Using this method, the variation trends of the sc_PDSI(P–M), P and ET_0 are examined by calculation of the Z value using all land grid cells from 1951 to 2015.

3. Results

3.1. Influence of ET_0 on sc_PDSI(P–M)

A Pearson correlation analysis was conducted between the sc_PDSI (P–M) and ET_0 (Fig. 2). On a one-month timescale, the sc_PDSI(P–M) had a low correlation with ET_0 and only a few areas in southern China showed a significant negative correlation. On a three-month timescale, there were far fewer areas with a significant negative correlation between the sc_PDSI(P–M) and ET_0. However, on a six-month timescale, there was a significant correlation in all areas of China, except for some parts of northwest and southwest China. There was a high negative correlation downstream of the Yellow River, in the Heilongjiang and Irtysh river basins, and north of the Greater Hinggan Mountains. On a 12-month timescale, there was a significant correlation throughout China, except for the Tarim and Qaidam basins. There was a high negative correlation in northeast and north China, south of the Yangtze River, and in the Brahmaputra and Nu river basins.

Taking into account the possible effects of trends in the mis-estimation of the correlation values, the detrended series were used to evaluate the links between the detrended sc_PDSI(P–M) and ET_0 (Fig. 3). Noticeable differences were seen between the original and detrended sc_PDSI(P–M) and ET_0 on a 12-month timescale, with a lower correlation than the original correlation in north China. This suggested that the variation in ET_0 had masked the tendency for a variation in

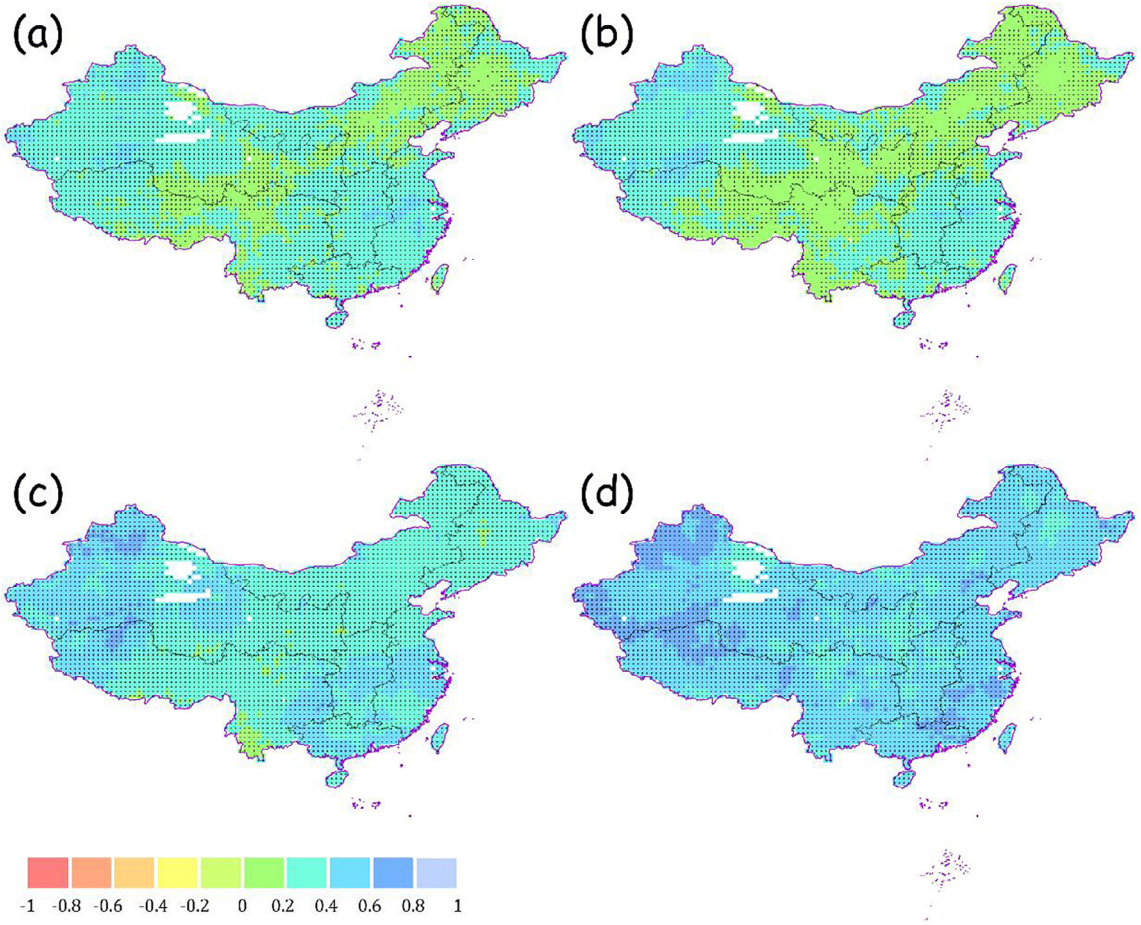

Fig. 4. Pearson's correlation coefficient between the self-calibrating Palmer Drought Severity Index using the FAO-56 Penman–Monteith equation (sc_PDSI(P–M)) and precipitation (P) on different timescales at the grid cell level in China during 1951–2015. The dotted areas are statistically significant at the 5% level. (a) One-month, (b) three-month, (c) six-month and (d) 12-month timescales.

droughts in this region, which is characterized by limited precipitation and high rates of evapotranspiration. The differences in correlation between the original and detrended data series were smaller on the other timescales.

3.2. Influence of P on the sc_PDSI(P–M)

A Pearson correlation analysis between the sc_PDSI(P–M) and P was also conducted (Fig. 4). On a one-month timescale, the sc_PDSI(P–M) showed a higher correlation with P in almost all of China, except for the line from the Greater Hinggan Mountains, north of the Loess Plateau, the Source Region of the Yangtze, Yellow and Lancang Rivers to the southeast of the Tibetan Plateau. On a three-month timescale, the areas showed an obvious reduction in the significant positive correlation on the same line. However, on a six-month timescale, there was a significant correlation in all of China and a high positive correlation south of the Yangtze River, the Pearl River basin, and the vast region of the Dzungarian Basin and Kunlun Mountains. On a 12-month timescale, the significant high correlation expanded to cover almost all regions of China. The highest positive correlation was in the Dzungarian Basin, the Kunlun Mountains and some parts of the Chang Jiang Downstream Plain.

The detrended series were also used to evaluate the links between the detrended sc_PDSI(P–M) and P (Fig. 5). Noticeable differences were seen between the original and detrended sc_PDSI(P–M) and P on a 12-month timescale, with a lower correlation than the original on the northern Tibetan Plateau. This suggested that the variation in P had masked the tendency for a variation in this region with high orographic precipitation. However, the differences in correlation between the original and detrended data series were smaller on other timescales.

4. Discussion

Based on the above findings, as the highest correlation between sc_PDSI(P–M) and ET_0 was seen on a 12-month timescale, an increased intensity of precipitation might be the cause of the non-significant correlation between the sc_PDSI(P–M) and ET_0 in some river basins, such as the Yangtze, Pearl and Tarim river basins (Piao et al., 2010; Wang and Zhang, 2011; Ren et al., 2015). The higher correlation between the sc_PDSI(P–M) and P may occur on either timescale, but on the 12-month timescale in particular. Specifically, the low correlations were only seen near the 400 mm precipitation contour on short timescales. This contour stretched from the Greater Hinggan Mountains in the northeast to the Himalaya in the southwest in mountainous areas where the precipitation has complex characteristics. On a 12-month timescale, the high correlation was seen in the Pearl River basin, downstream of the Yangtze River, and in the Altai, Tianshan and Kunlun mountains. In northwestern China, precipitation decreased from northwest to southeast, from the windward slopes (facing northwest) to the leeward slopes (facing southeast) and from mountainous areas to the basins (Li et al., 2011). The high mountains also received high orographic precipitation. Precipitation was abundant in southern China (e.g., the Pearl, Southeast and Yangtze river basins), with only small variations, and water resources were both sufficient and stable (Ren et al., 2015). Thus abundant precipitation might be a cause of the high sensitivity of the sc_PDSI(P–M) to P. Zhang et al. (2010) also

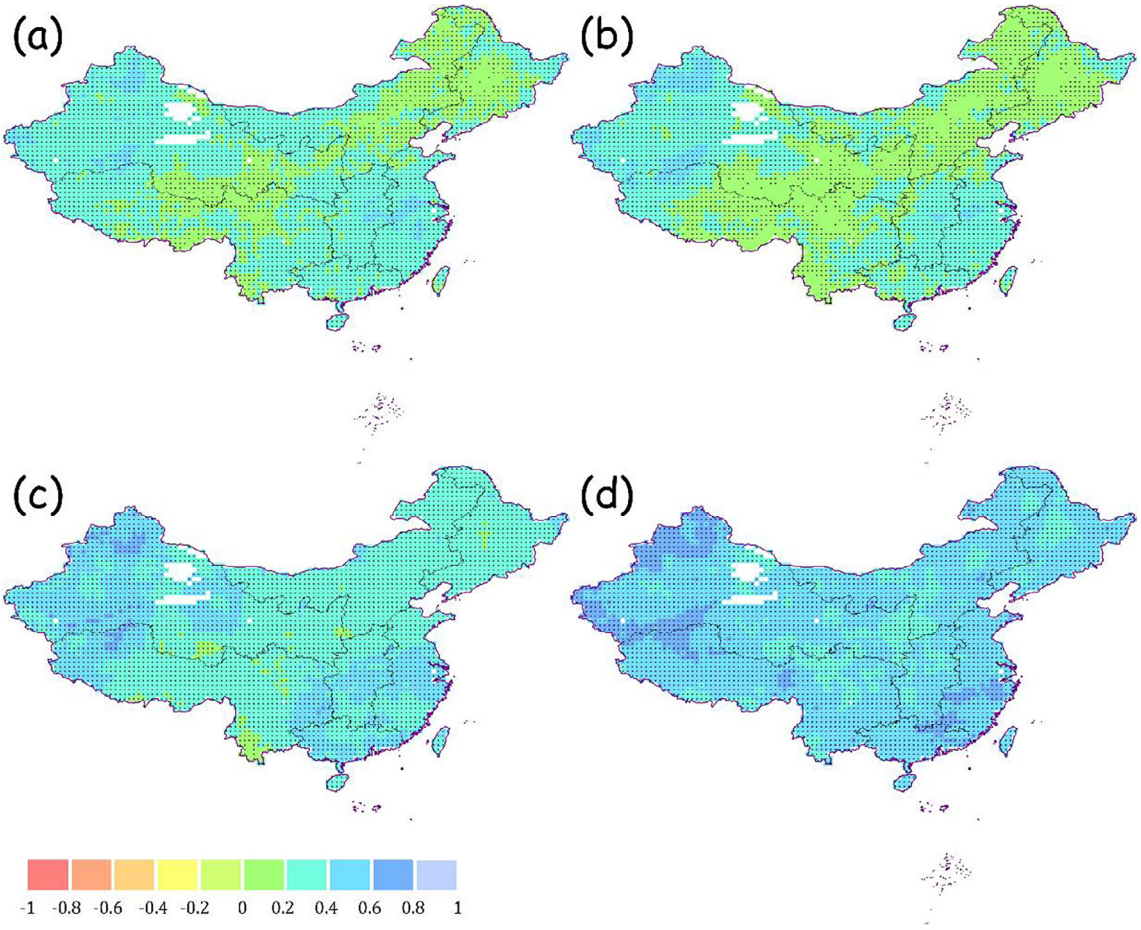

Fig. 5. Pearson's correlation coefficient between the detrended self-calibrating Palmer Drought Severity Index using the FAO-56 Penman–Monteith equation (sc_PDSI (P–M)) and detrended precipitation (P) on different timescales at the grid cell level in China during 1951–2015. The dotted areas are statistically significant at the 5% level. (a) One-month, (b) three-month, (c) six-month and (d) 12-month timescales.

confirmed that precipitation was the main factor causing drought in southwestern China. Taking the 12-month timescale as an example, the relationships between sc_PDSI(P–M) and P (and ET_0) in most areas of China might explained by the diverse hydroclimatic conditions and combined effects of P and ET_0 (e.g., the differences and different trends of change in sc_PDSI(P–M), P and ET_0) (Fig. 6) (Vicente-Serrano et al., 2015). The land surface might also play a more active role in the water cycle in these regions, indicating a strong influence of soil wetness on atmospheric stability (Qian and Leung, 2007).

Compared with the shorter timescales, the 12-month timescale was the most suitable timescale with which to verify the correlation of the sc_PDSI(P–M) with P and ET_0. This is because the calculation process for the sc_PDSI was organized with two intermediate variables (the moisture departure d and moisture anomaly index Z) and four parameters (climate characteristics K_1 and K_2, and duration factors p and q). Of these intermediate variables, d was the integrated output of eight hydrological variables in a two-layer water balance model computed at one-month time steps. K_1 was used to correct d with the second intermediate derived variable Z. This moisture anomaly index Z is known as the Palmer Z index, and may reflect the moisture condition of the current month (Heim, 2002). In the self-calibrating process, Wells et al. (2004) adopted 10 Z values accumulated at 3, 6, 9, 12, 18, 24, 30, 36, 42 and 48 months to represent extremely dry or extremely wet conditions. A linear regression equation was used to fit these extreme values. Based on the linear regression equation, the formulas of the two duration factors p and q could be derived using the accumulated Z values through a series of mathematical recursion processes, where p and q denote the correlation of the index to the preceding and current moisture status. If p is larger and q smaller, then the PDSI is less sensitive to sudden changes in precipitation. According to Palmer's scheme, the occurrence of a drought is an accumulative process and a current PDSI value could be computed as a weighted (i.e., duration factors) sum of the precedent PDSI value and the current moisture anomaly Z. Following these steps, a preliminary estimation of the PDSI values was obtained. This involved the calculation of the climate characteristic K_2 to make a secondary correction to the PDSI values and a back-tracking process to determine the termination or update of a drought/wet spell. During the calculation of the sc_PDSI, Liu et al. (2017) confirmed that the algorithm of duration factors estimation was probably related to the lengthened timescale of the sc_PDSI. It is accepted that the PDSI is typically computed for a single month, but the algorithm incorporates both precipitation and temperature data and the local available water content of the soil for an unspecified period, which commonly ranges from 9 to 18 months, but best corresponds to the most recent 9–12 months depending on the hydrometeorological characteristics of the region (Guttman, 1998; Heim, 2002; Keyantash and Dracup, 2002). Past conditions were incorporated because long-term drought is cumulative, so the intensity of drought at a particular time is dependent on the current conditions and the cumulative patterns of previous months.

Subsequently, the mean Pearson's correlation coefficient between the sc_PDSI(P–M) and P and ET_0 (and also between the detrended sc_PDSI(P–M) and detrended P and ET_0) were compared on different timescales and at different spatial scales (Figs. 7 and 8). The following results were obtained: (1) in the same region, the sc_PDSI(P–M) was highly correlated with P on a 12-month timescale, but poorly correlated

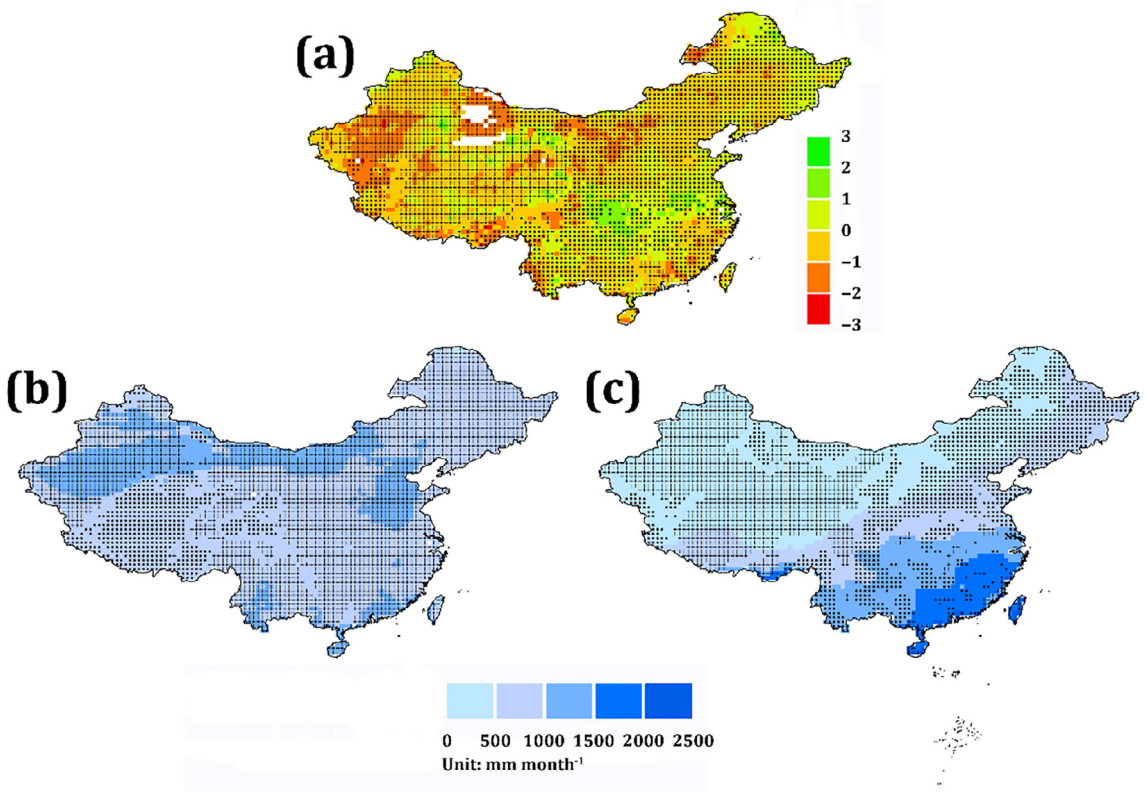

Fig. 6. Mean values and variation trends of (a) the self-calibrating Palmer Drought Severity Index using the FAO-56 Penman–Monteith equation, (b) the reference evapotranspiration and (c) precipitation on the 12-month timescale examined by the Mann–Kendall trend test at the grid cell level in China during 1951–2015. The + symbol represents an upwards trend with $p \leq 0.05$; ● represents a downwards trend with $p \leq 0.05$.

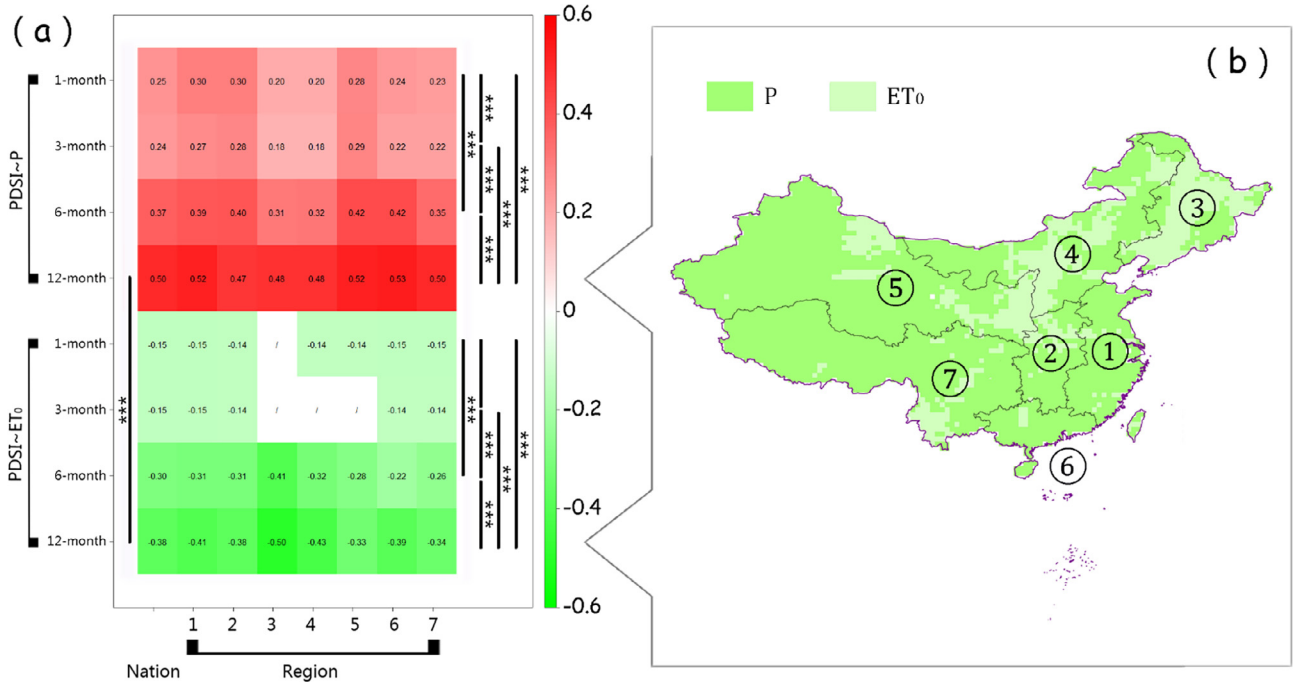

Fig. 7. (a) The mean Pearson's correlation coefficient between the self-calibrating Palmer Drought Severity Index using the FAO-56 Penman–Monteith equation (sc_PDSI(P–M)) and precipitation (P) and reference evapotranspiration (ET_0) on different timescales (one, three, six and 12 months) and at different spatial scales (national and seven regions of China) and (b) the dominant factor that mainly affected the sc_PDSI(P–M) calculated by ET_0 and P on a 12-month timescale at the grid cell level during 1951–2015 in China. One, two and three star(s) denote(s) the 90%, 95% and 99% confidence levels, respectively.

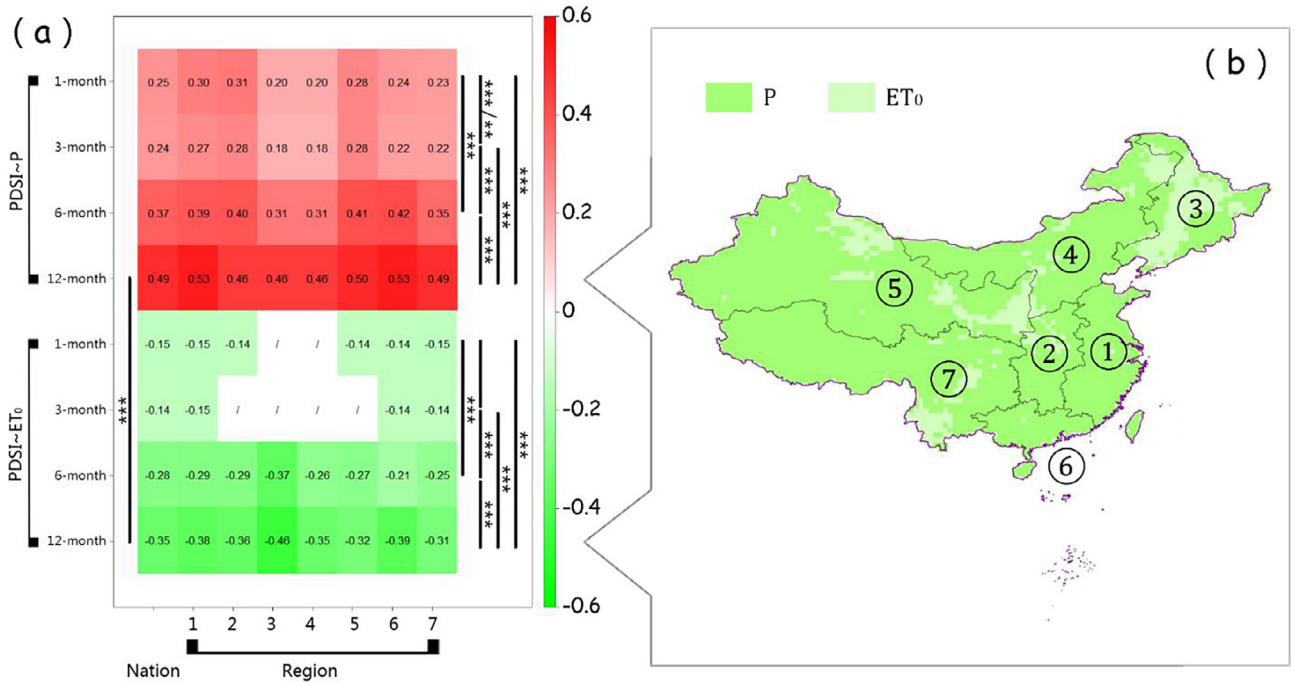

Fig. 8. (a) Mean Pearson's correlation coefficient between the detrended self-calibrating Palmer Drought Severity Index using the FAO-56 Penman–Monteith equation (sc_PDSI(P–M)) and detrended precipitation (P) and reference evapotranspiration (ET_0) on different timescales (one, three, six and 12 months) and at different spatial scales (national and seven regions of China) and (b) the dominant factor that mainly affected the detrended sc_PDSI(P–M) calculated by the detrended ET_0 and P on a 12-month timescale at the grid cell level in China during 1951–2015. One, two and three star(s) denote(s) the 90%, 95% and 99% confidence levels, respectively.

with P on a three-month timescale. There were statistically significant differences at the 0.001 level among these timescales; (2) the sc_PDSI (P–M) was highly correlated with ET_0 on a 12-month timescale, but poorly correlated with ET_0 on a three-month timescale in the same region. There were statistically significant differences at the 0.001 level among these timescales, except for a non-significant difference ($p > 0.05$) between the one- and three-month timescales; (3) an increasing trend was seen in the correlation between sc_PDSI(P–M) and P or ET_0 on medium and long timescales. There was a small discrepancy in the correlation analyses between the original and detrended sc_PDSI (P–M) and P and ET_0. The sc_PDSI(P–M) fitted the long-term variations in P and ET_0 and was highly correlated with these drivers of drought, especially on the 12-month timescale at the national and regional scales; and (4) higher correlations were found between sc_PDSI(P–M) and P than between sc_PDSI(P–M) and ET_0 on the same timescale in a particular region. On a 12-month timescale, the sc_PDSI(P–M) was more sensitive to P than to ET_0 and the difference was statistically significant at the 0.001 level on the national and regional scales, except in northeast China.

A comparison of the standardized regression coefficients of ET_0 and P on a 12-month timescale at the grid cell level in China during the time period 1951–2015 showed that the dominant factor influencing the sc_PDSI(P–M) nationally was P, except in some regions such as the Greater and Lesser Hinggan Mountains, the Northeastern Plain, the Loess Plateau, the Turfan Depression, the Qinling Mountains, the Taihang Mountains and the Yun-Gui Plateau. Vicente-Serrano et al. (2015) have shown that the sc_PDSI(P–M) is more sensitive to P than to ET_0, probably as a consequence of the standardization procedure for soil water budget anomalies. The actual evapotranspiration, which was included in the algorithm used to calculate the sc_PDSI(P–M), was limited by precipitation rather than ET_0. Dai et al. (2004) also showed that 70–90% of the variance in the PDSI was modulated by the variances in precipitation. The correlation of the sc_PDSI(P–M) with P was higher when $P > ET_0$, whereas the correlation between sc_PDSI(P–M) and ET_0 was stronger when the amplitude and variability of ET_0 were larger than the corresponding values of P (van der Schrier et al., 2013; Vicente-Serrano et al., 2015). However, there was no obvious spatial consistency between the pattern of water surplus and deficit (which showed a surplus in the south and a deficit in the northern and western parts of China) and the correlation of the sc_PDSI(P–M) with P and ET_0 during the period 1951–2015 (Gao and Xu, 2015). Thus the sc_PDSI (P–M) was not only driven by P and ET_0 because, in some regions, the correlation of sc_PDSI(P–M) with either P or ET_0 was clearly not high. There were three main reasons why the sc_PDSI(P–M) was weakly correlated with the drivers of drought in some cases. First, the procedure to standardize the moisture departure used in the sc_PDSI(P–M) strongly influenced the relationship between the sc_PDSI(P–M) and P and ET_0 (Wells et al., 2004). Second, a back-tracking criterion in the calculations of sc_PDSI(P–M), in which the determination of whether a dry or wet spell had ended would lead to a revision of previously computed values, diluted the direct relationship between the drought index and its drivers (Palmer, 1965; Wells et al., 2004; Vicente-Serrano et al., 2015). Third, in some mountainous regions, the glacial meltwater and snowmelt (delayed runoff) played an important part in runoff (Piao et al., 2010). However, this characteristic was not considered in the hydrological accounting section of the PDSI and might lead to a weak relationship between the PDSI and its climatic drivers (Liu et al., 2016).

Although the sc_PDSI requires many parameters in its complicated calculation process, the sc_PDSI(P–M) has been confirmed to closely track the soil moisture content and could be considered as a good indicator for monitoring and predicting long-term droughts and exploring the causes of drought, both worldwide and in China in particular (Dai et al., 2004; Szép et al., 2005; Zoljoodi and Didevarasl, 2013; Cook et al., 2015; Lu et al., 2015). Studies should be carried out to consider the influence of topography, climate and seasonal factors (e.g., winter soil freezing and thawing and spring snow melting) on the correlation of sc_PDSI(P–M) with P and ET_0 and to contribute to the worldwide application of the PDSI (and the sc_PDSI).

5. Conclusions

The sc_PDSI(P–M) was applied as an index for long-term drought monitoring in China to analyze its correlation with P and ET_0 using Pearson's correlation analysis with a detrending method on different timescales (one, three, six and 12 months) for the period 1951–2015. The results confirm that there is an increasing trend in the correlation of sc_PDSI(P–M) with P and ET_0 on medium and long timescales and that both P and ET_0 are highly correlated with sc_PDSI(P–M) on a 12-month timescale. This is because the sc_PDSI(P–M) is corresponds best to the most recent 12 months, as decided by the algorithm used for the estimation of duration factors in the calculation of the PDSI. The sc_PDSI (P–M) is therefore more sensitive to P than to ET_0 on a national scale, except in northeastern China, probably as a consequence of the standardization of anomalies in the soil water budget. The actual evapotranspiration estimated in the algorithm of sc_PDSI(P–M) was limited by precipitation rather than ET_0. Thus use of the PDSI is preferable for the estimation and quantification of long-term droughts in China.

Acknowledgments

The authors are indebted to Dong Gao at the College of Resources and Environment, University of Chinese Academy of Sciences, Beijing, for making suggestions. This study was funded through the National Key Research and Development Program of China (Grant No. 2016YFC0501803).

References

Allen, R.G., Pereira, L.S., Raes, D., Smith, M., 1998. Crop Evapotranspiration – Guidelines for Computing Crop Water Requirements. FAO Irrigation and Drainage Paper No. 56. FAO, Rome.

Bihrat, O.O., Bayazit, M.C., 2003. The power of statistical tests for trend detection. Turk. J. Eng. Environ. Sci. 27, 247–251.

Blaney, H.F., Criddle, W.D., 1950. Determining water requirements in irrigated area from climatologically irrigation data. US Department of Agriculture, Soil Conservation Service, Technology Paper No. 96.

Cook, B.I., Ault, T.R., Smerdon, J.E., 2015. Unprecedented 21st century drought risk in the American Southwest and Central Plains. Sci. Adv. 1, e1400082. https://doi.org/10.1126/sciadv.1400082.

Coumou, D., Rahmstorf, S., 2012. A decade of weather extremes. Nat. Clim. Change 2, 491–496.

Dai, A.G., 2011a. Drought under global warming: a review. Adv. Rev. 2, 45–65.

Dai, A.G., 2011b. Characteristics and trends in various forms of the Palmer Drought Severity Index during 1900–2008. J. Geophys. Res. 116, D12115. https://doi.org/10.1029/2010JD015541.

Dai, A.G., Trenberth, K.E., Qian, T.T., 2004. A global data set of palmer drought severity index for 1870–2002: relationship with soil moisture and effects of surface warming. J. Hydrometeorol. 5, 1117–1130.

Ding, Y., Hayes, M.J., Widhalm, M., 2011. Measuring economic impacts of drought: a review and discussion. Disaster Prev. Manage. 20, 434–446.

Gao, G., Xu, C.Y., 2015. Characteristics of water surplus and deficit change in 10 major river basins in China during 1961–2010. Acta Geog. Sin. 70, 380–391.

Guttman, N.B., 1998. Comparing the Palmer drought index and the standardized precipitation index. J. Am. Water Resour. Assoc. 34, 113–121.

Hanson, R.L., 1991. Evapotranspiration and Droughts. In: Paulson, R.W., Chase, E.B., Roberts, R.S., Moody, D.W., Compilers, National Water Summary 1988 – 89: Hydrologic Events and Floods and Droughts: U.S. Geological Survey Water-Supply Paper 2375. pp. 99–104.

Hargreaves, G.H., Samani, Z.A., 1985. Reference crop evapotranspiration from temperature. Trans. ASAE 28, 96–99.

Harris, I., Jones, P.D., Osborn, T.J., Lister, D.H., 2014. Updated high-resolution grids of monthly climatic observations – the CRU TS3.10 Dataset. Int. J. Climatol. 34, 623–642.

Hayes, M.J., Svoboda, M.D., Wilhite, D.A., 2000. Monitoring drought using the standardized precipitation index. In: Wilhite, D.A. (Ed.), Drought: A Global Assessment. Routledge, London, UK, pp. 168–180.

Hayes, M.J., Svoboda, M.D., Wilhite, D.A., Vanyarkho, O.V., 1999. Monitoring the 1996 drought using the standardized precipitation index. Bull. Am. Meteorol. Soc. 80, 429–438.

Heim, R.R., 2002. A review of twentieth-century drought indices used in the United States. Bull. Am. Meteorol. Soc. 83, 1149–1165.

Hobbins, M.T., Dai, A., Roderick, M.L., Farquhar, G.D., 2008. Revisiting the parameterization of potential evaporation as a driver of long-term water balance trends. Geophys. Res. Lett. 35, L12403. https://doi.org/10.1029/2008GL033840.

Hu, Q., Willson, G.D., 2000. Effect of temperature anomalies on the Palmer drought severity index in the central United States. Int. J. Climatol. 20, 1899–1911.

Keyantash, J., Dracup, J.A., 2002. The quantification of drought: An evaluation of drought indices. Bull. Am. Meteorol. Soc. 83, 1167–1180.

Kite, G.W., Droogers, P., 2000. Comparing evapotranspiration estimates from satellites, hydrological models and field data. J. Hydrol. 229, 3–18.

Li, X.M., Jiang, F.Q., Li, L.H., Wang, G.G., 2011. Spatial and temporal variability of precipitation concentration index, concentration degree and concentration period in Xinjiang, China. Int. J. Climatol. 31, 1679–1693.

Liu, W.W., An, S.Q., Liu, G.S., Guo, A.H., 2004. The farther modification of Palmer drought severity model. J. Appl. Meteorol. Sci. 15, 207–216.

Liu, Y., Ren, L., Hong, Y., Zhu, Y., Yang, X., Yuan, F., Jiang, S., 2016. Sensitivity analysis of standardization procedures in drought indices to varied input data selections. J. Hydrol. 538, 817–830.

Liu, Y., Zhu, Y., Ren, L., Singh, V.P., Yang, X., Yuan, F., 2017. A multiscalar Palmer drought severity index. Geophys. Res. Lett. 44, 6850–6858.

Lu, H.J., Mo, X.G., Liu, S.X., 2015. Intercomparison of three indices for addressing drought variability in North China Plain during 1962-2012. Hydrological Sciences and Water Security: Past, Present and Future 366, pp. 141–142.

Miyan, M., 2015. Droughts in asian least developed countries: vulnerability and sustainability. Weather Clim. Extremes 7, 8–23.

Nouri, M., Homaee, M., Bannayan, M., 2017. Quantitative trend, sensitivity and contribution analyses of reference evapotranspiration in some arid environments under climate change. Water Resour. Manage. 31, 2207–2224.

Palmer, W.C., 1965. Meteorological droughts. U.S. Department of Commerce Weather Bureau Research Paper. pp. 45, 58.

Penman, H.L., 1948. Natural evaporation from open water, bare soil and grass. Proc. R. Soc. London 193, 120–145.

Piao, S.L., Ciais, P., Huang, Y., Shen, Z.H., Peng, S.S., Li, J.S., Zhou, L.P., Liu, H.Y., Ma, Y.C., Ding, Y.H., Friedlingstein, P., Liu, C.Z., Tan, K., Yu, Y.Q., Zhang, T.Y., Fang, J.Y., 2010. The impacts of climate change on water resources and agriculture in China. Nature 467, 43–51.

Qian, Y., Leung, L.R., 2007. A long-term regional simulation and observations of the hydroclimate in China. J. Geophys. Res. 112, D14104. https://doi.org/10.1029/2006JD008134.

Rana, G., Katerji, N., 2000. Measurement and estimation of actual evapotranspiration in the field under Mediterranean climate: a review. Eur. J. Agron. 13, 125–153.

Ren, G.Y., Zhan, Y.J., Ren, Y.Y., Chen, Y., Wang, T., Liu, Y.J., Sun, X.B., 2015. Spatial and temporal patterns of precipitation variability over mainland China: I. Climatology. Adv. Water Sci. 26, 299–310.

Sheffield, J., Wood, E.F., Roderick, M.L., 2012. Little change in global drought over the past 60 years. Nature 491, 435–438.

Shen, C., Wang, W.C., Hao, Z., Gong, W., 2007. Exceptional drought events over eastern China during the last five centuries. Clim. Change 85, 453–471.

Szép, I., Mika, J., Dunkel, Z., 2005. Palmer drought severity index as soil moisture indicator: physical interpretation, statistical behaviour and relation to global climate. Phys. Chem. Earth 30, 231–243.

Thornthwaite, C.W., 1948. An approach toward a rational classification of climate. Geogr. Rev. 38, 55–94.

Trenberth, K., Dai, A., van der Schrier, G., Jones, P., Barichivich, J., Briffa, K., Sheffield, J., 2014. Global warming and changes in drought. Nat. Clim. Change 4, 17–22.

van der Schrier, G., Jones, P.D., Briffa, K.R., 2011. The sensitivity of the PDSI to the Thornthwaite and Penman–Monteith parameterizations for potential evapotranspiration. J. Geophys. Res. Atmospheres 116, 613–632.

van der Schrier, G., Barichivich, J., Briffa, K.R., Jones, P.D., 2013. A scPDSI-based global data set of dry and wet spells for 1901–2009. J. Geophys. Res. Atmospheres 118, 4025–4048.

Vicente-Serrano, S., Beguería, S., Lorenzo-Lacruz, J., et al., 2012. Performance of drought indices for ecological, agricultural and hydrological applications. Earth Interact 16, 1–27.

Vicente-Serrano, S., van der Schrier, G., Beguería, S., Azorin-Molina, C., Lopez-Moreno, J., 2015. Contribution of precipitation and reference evapotranspiration to drought indices under different climates. J. Hydrol. 526, 42–54.

Wang, S.R., Zhang, Z.Q., 2011. Effects of climate change on water resources in China. Clim. Res. 47, 77–82.

Wei, J., Ma, Z.G., 2003. Comparison of palmer drought severity index, percentage of precipitation anomaly and surface humid index. Acta Geog. Sinica 58, 117–124.

Wells, N., Goddard, S., Hayes, M.J., 2004. A self-calibrating palmer drought severity index. J. Clim. 17, 2335–2351.

Wilhite, D., Glantz, M., 1985. Understanding the drought phenomenon: the role of definitions. Water Int. 10, 111–120.

Xu, C.Y., Gong, L., Jiang, T., Chen, D., Singh, V.P., 2006. Analysis of spatial distribution and temporal trend of reference evapotranspiration and pan evaporation in Changjiang (Yangtze River) catchment. J. Hydrol. 327, 81–93.

Yu, S.C., Gao, G.L., 1991. Calculation and analysis to the field evaporation and drought. J. Hebei Agrotech. Teachers College 5, 44–52.

Zhai, J.Q., Su, B., Krysanova, V., Vetter, T., Gao, C., Jiang, T., 2010. Spatial variation and trends in PDSI and SPI indices and their relation to streamflow in ten large regions of China. J. Clim. 23, 649–663.

Zhang, D.Q., Zhang, L., Yang, J., Feng, G.L., 2010. The impact of temperature and precipitation variation on drought in China in last 50 years. Acta Phys. Sinica 59, 655–663.

Zhang, Q., 2003. Drought and its impacts. In: Chen, H. (Ed.), China Climate Impact Assessment (2002). China Meteorology Press, Beijing, pp. 12–18.

Zhang, Y.J., Li, Y., Ge, J., Li, G.P., Yu, Z.S., Niu, H.S., 2018. Correlation analysis between drought indices and terrestrial water storage from 2002 to 2015 in China. Environ. Earth Sci. 77, 462. https://doi.org/10.1007/s12665-018-7651-8.

Zhang, Y.J., Wang, Y.F., Niu, H.S., 2017. Spatio-temporal variations in the areas suitable

for the cultivation of rice and maize in China under future climate scenarios. Sci. Total Environ. 601–602, 518–531.
Zhao, Q., Wu, W.W., Wu, Y.L., 2015. Variations in China's terrestrial water storage over the past decade using GRACE data. Geod. Geodyn. 6, 187–193.
Zoljoodi, M., Didevarasl, A., 2013. Evaluation of spatial-temporal variability of drought events in Iran ssing Palmer Drought Severity Index and its principal factors (through 1951–2005). Atmos. Clim. Sci. 3, 193–207.
Zou, X.K., Zhai, P.M., Zhang, Q., 2005. Variations in droughts over China: 1951–2003. Geophys. Res. Lett. 32, L04707. https://doi.org/10.1029/2004GL021853.